

Wastewater microorganisms impact the micropollutant biotransformation potential of natural stream biofilms

Werner L. Desiante^{a,b}, Louis Carles^a, Simon Wullschleger^a, Adriano Joss^a, Christian Stamm^{a,b}, Kathrin Fenner^{a,b,c,*}

^a Eawag, Swiss Federal Institute of Aquatic Science and Technology, 8600 Dübendorf, Switzerland

^b Institute of Biogeochemistry and Pollutant Dynamics, ETH Zürich, 8092 Zürich, Switzerland

^c Department of Chemistry, University of Zürich, 8057 Zürich, Switzerland

ABSTRACT

Biotransformation is the most important process removing manmade chemicals from the environment, yet mechanisms governing this essential ecosystem function are underexplored. To understand these mechanisms, we conducted experiments in flow-through systems, by colonizing stream biofilms under different conditions of mixing river water with treated (and ultrafiltered) wastewater. We performed biotransformation experiments with those biofilms, using a set of 75 micropollutants, and could disentangle potential mechanisms determining the biotransformation potential of stream biofilms. We showed that the increased biotransformation potential downstream of wastewater treatment plants that we observed for specific micropollutants contained in household wastewaters (*downstream effect*) is caused by microorganisms released with the treated effluent, rather than by the in-stream exposure to those micropollutants. Complementary data from 16S rRNA amplicon-sequencing revealed 146 amplicon sequence variants (ASVs) that followed the observed biotransformation patterns. Our results align with findings for community tolerance, and provide clear experimental evidence that microorganisms released with treated wastewater integrate into downstream biofilms and impact crucial ecosystem functions.

1. Introduction

Establishing causal relationships between wastewater treatment plant (WWTP) effluents and effects on microbial community functions of the receiving aquatic ecosystems is challenging (Stamm et al. 2016). However, considering the increasing anthropogenic pollution impacting aquatic environments on a global scale, there is an urgent need to understand the mechanisms leading to functional changes of these crucial ecosystems (Caliman and Gavrilescu 2009, Gavrilescu et al. 2015, Posthuma et al. 2020). Treated effluent from WWTPs has, for instance, been recognized as one of the most dominant sources of antibiotic resistant bacteria and resistance genes to the environment (Collignon et al. 2018, Ju et al. 2019). Further, microbes released with treated effluent have been shown to increase organic matter decomposition downstream of WWTPs (Burdon et al. 2020). These observations raise the question whether the presence of treated effluent might also effect other carbon cycling-related processes such as the extent of removal of manmade chemicals from the environment through biodegradation.

Micropollutants (MPs) are manmade chemicals present in the environment in the low µg to ng/L range. They encompass many bioactive compounds, which might affect aquatic ecosystems, such as

pharmaceutical ingredients or pesticides released through various pathways such as WWTP effluents or agricultural runoff (Wen et al. 2017). While microbial biotransformation is recognized as the main contributor to the ultimate removal of MPs from water (Fenner et al. 2013), removal rates can vary significantly between microbial communities (Achermann et al. 2018b, Latino et al. 2017, Wang et al. 2018). Yet, factors leading to an increase or decrease of biotransformation are only partially understood.

In a previous field study, we investigated MP biotransformation in biofilms grown in rivers up- and downstream of two WWTP outfalls, where the upstream river sections received no wastewater input, to explore how exposure history impacts MP biotransformation (Desiante et al. 2021). For a specific subset of compounds, we found an increased biotransformation potential in the downstream biofilm communities compared to the upstream ones (i.e., a '*downstream effect*'). A similar effect has previously been observed for the artificial sweetener acesulfame in biotransformation studies with river sediments (Coll et al. 2020). We concluded that understanding the spatial and temporal extent of increased biotransformation as well as the nature of MPs actually showing a *downstream effect* is essential to properly assess the risk related to the release of MPs to the aquatic environment. We

* Corresponding author.

E-mail address: kathrin.fenner@eawag.ch (K. Fenner).

<https://doi.org/10.1016/j.watres.2022.118413>

Received 18 October 2021; Received in revised form 31 March 2022; Accepted 4 April 2022

Available online 7 April 2022

0043-1354/© 2022 The Author(s). Published by Elsevier Ltd. This is an open access article under the CC BY-NC license (<http://creativecommons.org/licenses/by-nc/4.0/>).

hypothesized that the *downstream effect* was either due to the presence of MPs in the WWTP effluent, or due to the immigration of microorganisms released from the high-load activated sludge compartment of WWTPs. Depending on the actual mechanism, the relevance of the *downstream effect* may differ substantially. Given the ubiquitous presence of MPs in streams impacted by urban and agricultural wastewater, it is perceivable that in-stream effects of chemicals may extend over long distances. Contrastingly, if functional changes are mainly induced by the release of adapted microorganisms, their spatial extent might be more limited. While for AR the longitudinal effect has recently been shown to decrease rapidly (Lee et al. 2021), such data is missing for biotransformation of MPs.

In the present study, we set out to elucidate the mechanisms underlying the increased MP biotransformation potential of biofilms grown downstream of WWTP outfalls relative to upstream biofilms ('*downstream effect*'). In support of such mechanistic understanding, we further asked what the compounds showing a *downstream effect* had in common. We additionally aimed to set our findings in relation to another ecologically relevant endpoint studied in the same series of experiments, i.e., the increased tolerance of downstream communities towards toxic MPs (Carles et al. 2021, Tlili et al. 2016). Therefore, in a first experiment, we attempted to reproduce the field observations reported in Desiante et al. (2021) under controlled conditions in an experimental flume system in which stream biofilms were cultivated at different ratios of river water and treated wastewater (WW). We then investigated the biotransformation capacity of these biofilms toward a pre-defined set of 75 MPs ('*study compounds*'). We chose the *study compounds* in our experiments such as to include a structurally diverse set of wastewater-borne and non-wastewater-borne MPs to reveal if observed effects relate to specific (physico-)chemical or structural properties of the compounds and/or to specific exposure situations, and to discuss potential enzymatic pathways. In a second experiment, we modified the system in order to remove particles and microbes from WW, while keeping the other physicochemical parameters (i.e., MP concentrations, nutrients, temperature, etc.) as constant as possible. This allowed us to disentangle the effects of exposure to MPs and exposure to wastewater-borne microorganisms on biofilm MP biotransformation potential, while excluding influences from other factors. Concomitantly, we monitored influent and effluent MP concentrations of the WWTP producing the treated effluent for our experiments in order to compare removal of MPs in the WWTP to their biotransformation in the biofilms. Finally, we analyzed differences in the community composition in order to highlight taxa whose abundance patterns align with the *downstream effect*.

2. Materials and methods

2.1. Overview

In order to cultivate stream biofilms, an indoor version of the Maiandros experimental flow-through channel system, described by Burdon et al. (2020), was used. The biofilms grown in the channel system were then used to perform two biotransformation experiments (Exp 1 and Exp 2). To do so, biofilms were suspended, spiked with a mixture of 75 MPs ('*study compounds*'), and sampled over the duration of the experiments.

2.2. Maiandros experimental system Exp 1

The experimental channel system Maiandros, used to cultivate stream biofilms for Exp 1, was described thoroughly by Burdon et al. (2020) and by Carles et al. (2021) for changes specific to the indoor iteration. Briefly, the experimental system, consisting of 16 equivalent flow-through channels, was fed with two sources of water, i.e., river water and treated wastewater (WW). A lighting system that reproduces the sunlight spectrum (Philips Master LED tube HF 1200 mm) was

installed to ensure a photoperiod of 12h light and 12h dark. The WW for this setup was produced in a pilot-size wastewater treatment plant (100 person equivalents) using standard activated sludge treatment for nitrification and denitrification, with the influent originating from a municipal sewer in the catchment of Dübendorf, Switzerland. The river water derived from a small, peri-urban stream (Chriesbach; Dübendorf, Switzerland). The treatments in the channels were adjusted to nominal concentrations of 0% (control treatment), 10%, 30% and 80% WW, mixed in with river water, resulting in four biological replicates per treatment (0% WW, 10% WW, 30% WW and 80% WW, respectively). Manual adjustment of the treatment concentrations in the channels was done on a daily basis. The treatments were randomly distributed in the 16 channels to avoid block effects and minimize systematic external influences. Biofilms were allowed to grow in the water-fed channels on supporting glass slides for a period of four weeks from 19th of June to 15th of July 2019. During biofilm colonization, water parameters (pH, temperature, conductivity and dissolved oxygen) were measured manually on a daily basis in the 16 channels, and 20 water quality parameters were monitored weekly. Additionally, during the colonization phase, 52 organic micropollutants originally selected by Munz et al. (2017), 30 of which were overlapping with the *study compounds*, were monitored in the 16 channels, in the two water sources, and in the biofilms (Carles et al. 2021). Further information on the experimental system are given in (Carles et al. 2021).

2.3. Maiandros experimental system Exp 2

The second experiment (Exp 2) was conducted using a modified version of the system used for Exp 1. One major change was the installation of an ultrafiltration (UF) unit with a nominal pore size of 0.4 µm, allowing for the removal of particulates, including microorganisms, from WW. Thus, in this system, we had three sources of water, i.e., river water, WW, and ultrafiltered WW. Further, four additional flow-through channels were added to the system, resulting in 20 channels in total. The water sources were used to create five treatment conditions in the channels, consisting of 0% (control treatment), 30% and 80% WW, and 30% and 80% ultrafiltered WW mixed in with river water, resulting in four biological replicates per treatment (0% WW, 30% WW, 80% WW, 30% UF and 80% UF, respectively). Different from Exp 1, the mixing ratios in the channels were controlled automatically based on on-line conductivity probes of the three water sources. Biofilms were allowed to grow in the water-fed channels on supporting glass slides for four weeks from 11th of February to 9th of March 2020. During biofilm colonization, water parameters (pH, temperature, conductivity and dissolved oxygen) were measured manually on a daily basis in the 20 channels (SI section S1.2 and Table Appendix A1), and 20 water quality parameters were monitored weekly, using standard methods (SI sections S1.2 and S1.5 and Table Appendix A2) (FOEN 2020). Additionally, the same 52 organic micropollutants as in Exp 1 were monitored in the 20 channels, in the river and WW sources, before and after ultrafiltration, and in the biofilms (SI sections S1.3, S1.4 and Tables Appendix A3 – A7). A full description of the experimental flow-through channel system used for Exp 2 can be found in the SI section S1.1.

2.4. Study compounds

For the biotransformation experiments, a micropollutant mixture of 75 compounds was prepared, referred to as *study compounds*. The *study compounds* were chosen based on previous work (Desiante et al. 2021). They comprised multiple use classes (i.e., antibiotics, anti-corrosion agents, artificial sweeteners, fungicides, herbicides, insecticides and pharmaceuticals; Table S1), and were chosen because of their relevance to surface waters, i.e. potential exposure and/or potential toxic effects to aquatic organisms. In order to explore how exposure to MPs influences the biotransformation potential of stream biofilms, we chose the *study compounds* such that roughly half of the compounds typically occur in

wastewater, while the rest of the compounds typically are thought to enter the aquatic environment via different pathways (e.g., run-off from agricultural fields). Moreover, the *study compounds* were chosen to cover a broad range of molecular structures and, thus, potential initial biotransformation reactions (Desiante et al. 2021). HPLC grade chemicals were purchased from Sigma-Aldrich GmbH, Honeywell Specialty Chemicals, HPC Standards GmbH, Dr. Ehrenstorfer GmbH, and Toronto Research Chemicals. The 75 *study compounds* were combined in a spiking mix in EtOH (1 mg/L). For analysis, a mixture of 178 labelled internal standards (25 µg/L in EtOH) was spiked to the samples and assigned to the respective *study compounds*. A complete list of the *study compounds* and assigned internal standards is given in Table S1.

2.5. Biotransformation experiments

The two biotransformation experiments (Exp 1 and 2) were conducted in a similar manner as described in Desiante et al. (2021). Briefly, biofilms grown on five glass slides (210×75×4 mm per slide) from one channel (i.e., one biological replicate) were scraped off the glass slides and combined to form a stock suspension in artificial river water, i.e., periquil (Stewart et al. 2015). Standardization to similar biomass concentrations was done by optical density (OD) measurements at 685 nm, and by further diluting samples with higher biomass. From these stock suspensions, subsamples of 120 mL, 110 mL, and 120 mL were taken for the biotransformation experiment (BT), a sorption control (SC) and a biological control (BC), respectively. BC batches were used to investigate the influence of the spiked MPs on biofilm growth. Additionally, abiotic controls (AC), consisting of only artificial river water, were prepared. SC and AC batches were autoclaved (121°C, 2 bar, 20 min) before the start of the experiment. The experiments were conducted at 16°C. BT and BC batches were exposed to a 12 h light-dark cycle (Philips 10NC MAS LEDtube Value HF 1200 mm 16.5W865; 1600lm each; 865 Cool daylight; Photosynthetic Photon Flux Density (PPFD): 100 - 130 µmols⁻¹m⁻² at the height of the vessels). To start the experiment, 100 µL of spiking mix was added to each BT, SC and AC experimental vessel, resulting in a final concentration of approximately 1 µg/L of each substance (Table S1), while the BC batches were spiked with the same amount of pure EtOH. All experimental vessels were placed on laboratory shakers and shaken circularly at 150 rpm. Aqueous samples (1.5 mL) of the BT batches were taken before and at approximately 0, 1, 2, 4, 8, 24, 48, 72 and 96 hours after the start of the experiment, while samples of the SC and AC batches were taken before and at approximately 0, 4, 24, 48 and 72 hours after the start of the experiment. Samples were centrifuged (15 min, 4°C, 21'130 g), the supernatant (1 mL) was transferred into an amber HPLC vial, spiked with 20 µL internal standard mix to a concentration of 0.5 µg/L and then immediately frozen (-20°C) until analysis. Biofilm samples for determining solid phase concentrations were taken from the stock suspensions (before the start of the experiment), and at 48 and 96 h after the start of the experiment for the BT batches and at 48 and 72 h for the SC batches in Exp 1, and at 24, 48 and 96 h for the BT batches and at 24, 48 and 72 h for the SC batches in Exp 2, respectively. To do so, 10 mL of the suspension were sampled, centrifuged (15 min, 23°C, 3'800 g), the supernatant discarded and the pellet frozen (-80°C) until further extraction.

2.6. Biofilm extraction

In order to determine solid phase concentrations, the QuEChERS extraction method described in Desiante et al. (2021) was used. Briefly, lyophilized biofilm samples were spiked with a mix of isotope-labelled standards to correct for losses during extraction, sample processing and measurement. ACN/ultrapure H₂O were then added to the sample to result, upon phase-separation, in an ACN extract, which was stored at -20°C until evaporation under N₂. Consecutively, the residue was redissolved in 1000 µL ultrapure H₂O and measured by means of mass spectrometry. Further information on evaluation of solid phase

concentrations can be found in SI section S2.1.

2.7. WWTP sampling

During the biofilm colonization phase of Exp 1, a three-day time-proportional composite sample of the WWTP influent was taken between 8th – 11th of July 2019 and a four-day composite sample of the effluent between 7th – 11th of July 2019. During Exp 2, three weekly time-proportional composite samples of the WWTP influent, effluent and the ultrafiltered effluent were taken between 11th of February – 10th of March 2020, which were later combined to three-week composite samples. After sampling, the samples were immediately frozen (-20°C). Before HRMS analysis, the samples were allowed to thaw at 4°C overnight, 10 mL subsampled into 15 mL centrifuge tubes and centrifuged (20°C, 3800 g, 15 min). From these, 1 mL subsamples were pipetted into amber HPLC vials and spiked with 20 µL of the internal standard mix. Further information on the WWTP and evaluation of WWTP samples can be found in SI section S3.

2.8. Micropollutant analysis

In order to determine chemical concentrations, the same procedure as described in Desiante et al. (2021) was used. Briefly, reverse phase liquid chromatography coupled to a QExactive Plus (Thermo Scientific) was used to gather positive and negative full-scan MS spectra. Samples taken at 0 h after spiking were measured three times (technical triplicates) for every biological replicate. Micropollutant data analysis was performed according to Desiante et al. (2021). Target quantification for the 75 *study compounds* was done using the software Tracefinder 4.1 (Thermo Scientific). Technical triplicate measurements were used to calculate the analytical error of the measurements. Further data evaluation of experimental data was conducted in R version 3.6.1 (R Core Team 2017). Figures of concentration-time series were produced using the package ggplot2 (Wickham 2016). Concentration-time series were used to calculate first-order rate constants (k_{bio}) for every single biological replicate, assuming pseudo first-order kinetics, which were then averaged in order to obtain k_{bio} values for the investigated treatments (see Tables S2 and S3 for k_{bio} values of biotransformed compounds). R^2 was used as quality indicator of the fit. For visualization, linear regression models were fitted to the log-transformed values of the normalized data (c/c_0 , i.e., the measured concentration divided by the starting concentration) including all replicates ($n = 4$) of each treatment. Concentration-time series of all evaluated *study compounds* and linear regression plots for the *study compounds* that have been primarily biotransformed are displayed in Figures S7 and S8. Solid phase concentrations measured in biofilm samples were used to evaluate mass balances (Figures S9 and S10). Based on these, dominant fate processes were assigned to each compound as described in Desiante et al. (2021) (SI section S2.1). In order to compare biotransformation trends across the biotransformed chemicals and the biofilm communities, we level-normalized the calculated k_{bio} for each chemical across treatments and created heatmaps using the R package pheatmap (Kolde 2015, van den Berg et al. 2006).

2.9. Bacterial abundance quantification by flow cytometry

During the biofilm colonization phase of Exp 2, six samples for flow cytometry were taken from the treated wastewater buffer tank (WW) and directly after ultrafiltration (UF) on day two, nine, 16, 19, 21 and 23 after starting the colonization. During the biotransformation experiments Exp 1 and Exp 2, samples of the BT and BC batches were taken right before spiking and at 48 and 96 h. The sample processing and measurements were conducted in the same way as described in Desiante et al. (2021). Briefly, 5 mL of the samples were fixated with 5 mL buffer solution (4% paraformaldehyde + 0.2 % sodium pyrophosphate) in glass vials and stored at 4°C. After ultrasonication (4×20s), the samples were diluted, stained with 1% SYBR® Green (1:100 dilution in DMSO) and incubated at 37°C for 10 min. Measurements were conducted on a BD

Accuri C6® flow cytometer (BD Accuri, San Jose CA, USA). Flow cytometry data processing and analysis was done with the BD Accuri™ C6 Analysis software. Obtained total cell counts were used for graphical representation in R version 3.6.1 with the package ggplot2 (R Core Team 2017, Wickham 2016). For bacterial abundance time patterns, please see SI sections S2.3 and S2.4.

2.10. Total biomass quantification (ash-free dry mass, AFDM)

Sampling for total biomass quantification was done prior to and after 96 h in Exp 1 and after 48 and 96 h in Exp 2, for the BT and BC, respectively. To do so, 10 mL of the suspension were filtered over pre-equilibrated and pre-weighed 47 mm glass microfiber filters (GF/F grade, Whatman®, Maidstone, United Kingdom). Filters were dried in a ventilated oven (105°C) and allowed to equilibrate in a desiccator, before weighing again in order to determine the dry mass. Filters were then wrapped in aluminum foil, muffled (80 min heating up to 450°C, 1h at 450°C, cool down), allowed to equilibrate and weighed again in order to determine the weight of the mineral residues. Total biomass (i.e., AFDM) data analysis was done according to standard procedure. The determined weight of the mineral residues was subtracted from the determined dry mass in order to obtain the AFDM. The determined AFDM values were used for graphical representation in R version 3.6.1 with the package ggplot2 (R Core Team 2017, Wickham 2016). For total biomass growth patterns, please see SI sections S2.3 and S2.4.

2.11. Data analysis and statistics

In order to assess how much the *treatment* or the *biomass* (expressed as bacterial abundance or total biomass) accounted for the variability in k_{bio} across the different biofilm communities, we compared the predictive performance (R^2) of different linear regressions models for the logarithmized k_{bio} ($\log(k_{bio})$). We fitted linear regressions with *treatment*, *cells* and *AFDM* as explanatory variables, in the following combinations:

| Model | treatment | cells | AFDM |
|-------|-----------|-------|------|
| 1 | X | x | |
| 2 | | x | |
| 3 | X | | x |
| 4 | | | x |
| 5 | X | | |

where *treatment* stands for one of the nine individual treatments of both Exp 1 and Exp 2, *cells* for the bacterial abundance at 0 h determined by flow cytometry for individual biological replicates ($n = 4 \times 9$), and *AFDM* for the total biomass at 0 h for individual biological replicates ($n = 4 \times 9$). We then compared goodness of fit (R^2) between the models. If the difference in R^2 between a model containing both *treatment* and *biomass* compared to a model containing only one of the explanatory variables is small, we can conclude that the respective single explanatory variable (i. e., *treatment*, *cells*, or *AFDM*) explained the larger part of the variability in the model with two explanatory variables, and vice versa for large differences in R^2 . In order to assess the individual contribution of *treatment* and *cells* to the model containing both of these explanatory variables, we compared R^2 of model (1) with R^2 of models (2) and (5). Analogously, to assess the individual contribution of *treatment* and *AFDM* to the model containing both of these explanatory variables, we compared R^2 of model (3) with R^2 of models (4) and (5). Thus, we were able to separate the effect of *treatment* from the effect of *biomass*. For graphs visualizing models (2), (4) and (5) and a table containing the calculated R^2 values for all models, see SI section 2.2. Models were fitted using R version 3.6.1 (R Core Team 2017).

2.12. 16S rRNA amplicon sequencing

Total genomic DNA was extracted from an aliquot of 2 mL from each biofilm suspension after 4 weeks of colonization, and from 100 mL WW samples taken regularly (12 sampling times) during biofilm colonization by using the DNeasy PowerBiofilm Kit (QIAGEN) following the manufacturer's instructions. The biofilm samples were centrifuged at 14'000 g for 30 min at 4°C and the pellets stored at -80°C until their analyses. The sampling of wastewater during Exp 1 is described in Carles et al. (2021). During Exp 2, composite wastewater samples were taken regularly and immediately filtered on Supor® polyethersulfone membrane disc filters with 0.2 µm pore size (Pall Corporation, USA). The filters were stored at -80°C and cut in small pieces prior to DNA extraction. The library construction consisted in a two-step PCR process. Briefly, the first PCR amplified the V3-V4 region of the 16S rRNA gene using the primer set described by Herlemann et al. (2011). The second PCR was carried out to add multiplexing indices and Illumina sequencing adapters. The libraries were then normalized, pooled and sequenced (paired end 2×300 nt, Illumina MiSeq) following the manufacturer's run protocols (Illumina, Inc.). All raw sequences are available at the National Center for Biotechnology Information (NCBI) under the SRA accession IDs PRJNA699298 (Exp 1) and PRJNA755072 (Exp 2). Sequencing data processing, Amplicon Sequence Variants (ASVs) binning and taxonomic assignment were done according to Carles et al. (2021). Briefly, the reads were checked for quality and end-trimmed by using FastQC v0.11.2 (Andrews 2010) and seqtk (https://github.com/lh3/seqtk), respectively, and then merged using FLASH v1.2.11 (Magoč and Salzberg 2011). The primers were trimmed by using cutadapt v1.12 (Martin 2011). Quality filtering was performed with PRINSEQ-lite v0.20.4 with a subsequent size and GC selection step (Schmieder and Edwards 2011). The reads were processed with an Amplicon Sequence Variants (ASV) analysis (Callahan et al. 2017). The sample reads were first denoised into ASVs with UNOISE3 in the USEARCH software v.11.0.667. The final predicted taxonomic assignments were performed with SILVA v128 by using SINTAX in the USEARCH software v.11.0.667 (Edgar, 2016). The total number of reads obtained at each bioinformatics step is reported in Table S5.

An untargeted sequencing data analysis was performed in order to identify taxa that were transferred from the WWTP into biofilms and whose abundance patterns followed the *downstream effect* observed in the biodegradation experiments. The selection was based on the following criteria (see SI, Section S4 for the details): (1) the ASVs detected in biofilm at the end of the colonization period were also found in the wastewater effluent (Exp 1 & 2), (2) their abundance was significantly higher in 80% WW biofilms than in control (Exp1 & 2), (3) they were detected in both experiments, and (4) their abundance was significantly reduced by ultrafiltration (Exp 2). Applying these criteria, we selected a total of 135 and 146 taxa from Exp 1 and 2, respectively (Figure S31).

Additionally, a targeted analysis was also carried out to identify taxa with high sequence similarity to species previously reported to degrade compounds showing the *downstream effect*. More information on methods and results of the targeted analysis are provided in the SI, Section S4.

3. Results

3.1. Biotransformation of specific MPs depends on proportion of WW

In the first set of experiments (Exp 1), biofilms grown at four different treatment conditions (0%, 10%, 30% and 80% nominal treated wastewater (WW) concentration in the receiving channels) were used to conduct biotransformation batch experiments with the 75 *study compounds*. Experimental performance has already been evaluated and discussed in (Carles et al. 2021) and is summarized in SI section S1.4. Of the 75 *study compounds*, 38 were predominantly biotransformed, rather than mostly sorbed or bio-accumulated (see SI section S2.1.1). For those, we calculated biotransformation rate constants (k_{bio}) by fitting a first-order kinetic model to their concentration-time series (see Fig. 1 for the examples of acesulfame and caffeine and Figures S7 and S8 for the remaining compounds). The calculated

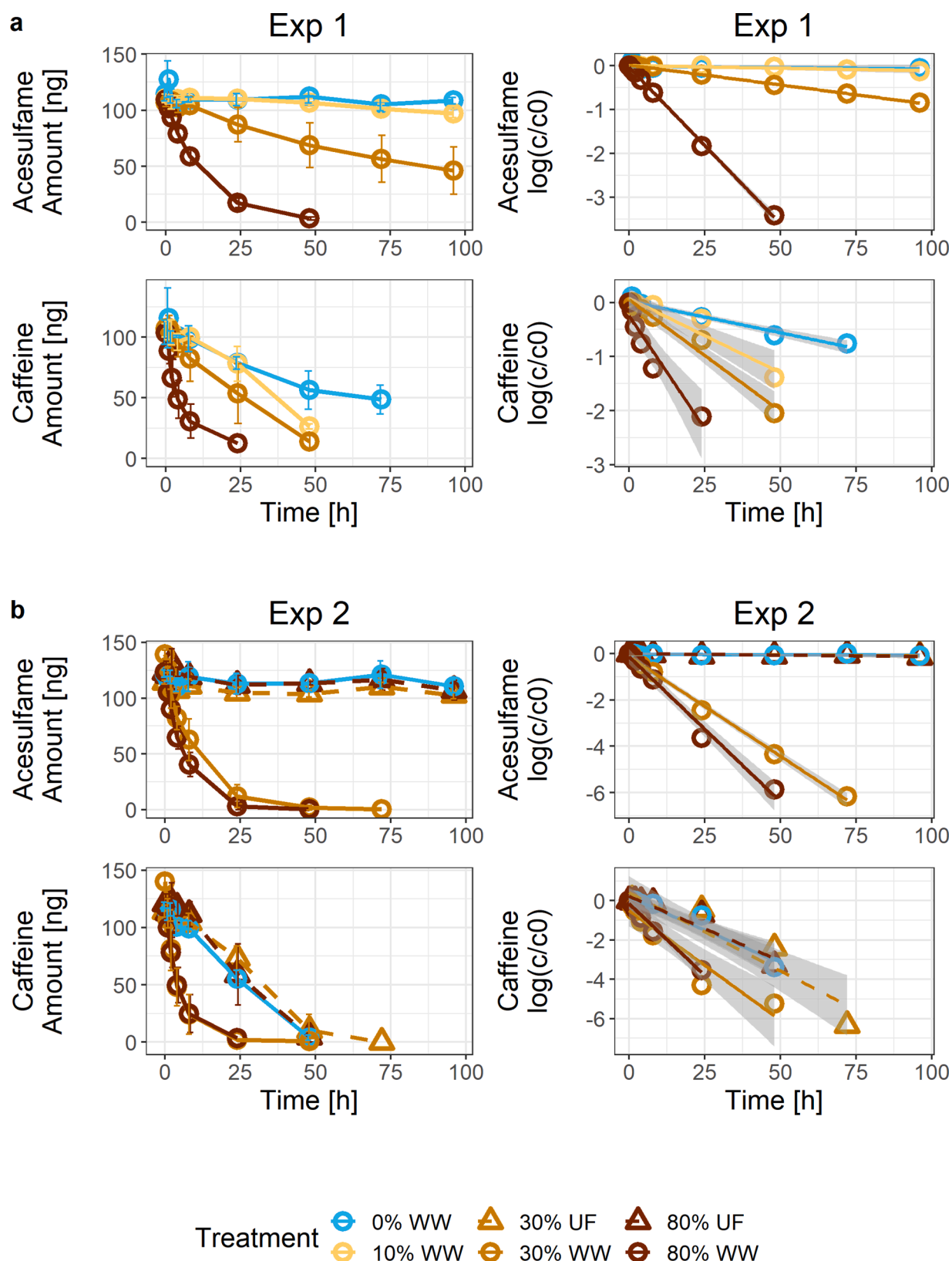


Fig. 1. Concentration-time series of the compounds acesulfame and caffeine in Exp 1 and 2. a) Data from biotransformation Exp 1. b) Data from biotransformation Exp 2. Ultrafiltered (UF) samples are displayed with triangles and dashed lines, while the other samples (WW) are displayed as circles and solid lines. Measured concentrations are given as absolute amount (ng) (left panels). Values are displayed as mean \pm standard deviation ($n = 4$). Lines in the left panels connect the mean values. The log-transformed data (c/c_0 , i.e., the measured concentration divided by the starting concentration) are displayed in the right panels. Lines represent the linear regression for each treatment across all replicates ($n = 4$). Gray bands correspond to the 95% confidence interval for the prediction of the linear regression model. Values are displayed as mean ($n = 4$).

k_{bio} values for all 38 biotransformed compounds are given in Tables S2 and S3. In Exp 1, for the example of acesulfame, no significant concentration decrease was observed in the 0% and 10% WW treatments, while we saw a sudden onset of biotransformation in the 30% WW treatment and an even faster removal of the compound in the 80% WW treatment (Fig. 1a). A similar pattern of increasing biotransformation with increasing proportion of WW was also observed for the compound caffeine, which, however, was already biotransformed to some extent in the control biofilms (0% WW) (Fig. 1a). Besides acesulfame and caffeine, nine more out of the 38 biotransformed compounds (i.e., the artificial sweeteners cyclamate and saccharin, the insect repellent DEET, and the pharmaceuticals cilastatin, eprosartan, furosemide, ketoprofen, levetiracetam and valsartan) showed a similar pattern of increased biotransformation at increased amounts of WW, albeit the exact onset of increased biotransformation in terms of % WW differed between compounds (SI section S2.1.6).

3.2. Ultrafiltration prevents the downstream effect

To distinguish the effect of increased MP concentrations from the potential influence of microorganisms released with the treated WW, the second set of experiments (Exp 2) included treatments at 30% and 80% WW in which the treated WW was subjected to ultrafiltration (UF) before being fed into the flow-through channels. This resulted in biofilms grown for four weeks at five different treatment conditions (0% WW, 30% WW, 30% UF, 80% WW and 80% UF, where UF stands for WW that has additionally been passed through the UF unit). These biofilms were then again used in batch experiments to study biotransformation of the 75 study compounds. Experimental performance of Exp 2 is discussed in SI S1.5. Analysis of concentration-time series and resulting rate constants from Exp 2 revealed a number of striking patterns. We found that seven out of the eleven

compounds having shown a dependence on the proportion of WW in Exp 1 (i.e., acesulfame, caffeine, cyclamate, DEET, levetiracetam, saccharin and valsartan), exhibited strong responses to the UF treatment (i.e., a reduction of the average k_{bio} for those seven compounds from 4.2 and 4.0 day^{-1} in the 30 and 80% WW treatments to 0.8 and 0.4 day^{-1} in the 30 and 80% UF treatments, compared to 0.6 day^{-1} in the 0% WW control treatment). This is again exemplarily illustrated in terms of the actual concentration-time series and kinetic fits for acesulfame and caffeine in Fig. 1b. As can be seen in Fig. 1b, acesulfame again was persistent in the control treatment (0% WW), but was removed in the 30% and 80% WW treatments. Yet, strikingly, ultrafiltration (30% and 80% UF) reversed this effect to the extent that no observable acesulfame biotransformation occurred in the UF treatments. A similar pattern was found for caffeine. While it was removed to a small degree in the control, higher removal was observed in the WW samples, but ultrafiltration (30% and 80% UF) prevented the effect of WW to similar levels of removal as observed in the control. These results suggest that the *downstream effect* must result from particle-bound traits that are released by the WWTP, yet filtered out by ultrafiltration in Exp 2. As the pore size of the ultrafiltration membrane ranges around 0.4 μm , it is highly unlikely that DNA fragments are removed in this step, but rather bacteria and larger sludge particles.

3.3. Treatment, not biomass amount, dictates biotransformation potential of compounds showing the downstream effect

In order to control for effects of biomass and treatment conditions on biotransformation, we determined total biomass and bacterial abundance in the biofilm suspensions prepared for the biotransformation experiments (Fig. 2). For the biofilm suspensions prepared for Exp 1, we determined a mean total biomass (AFDM) of 0.66 ± 0.12 g/L across all

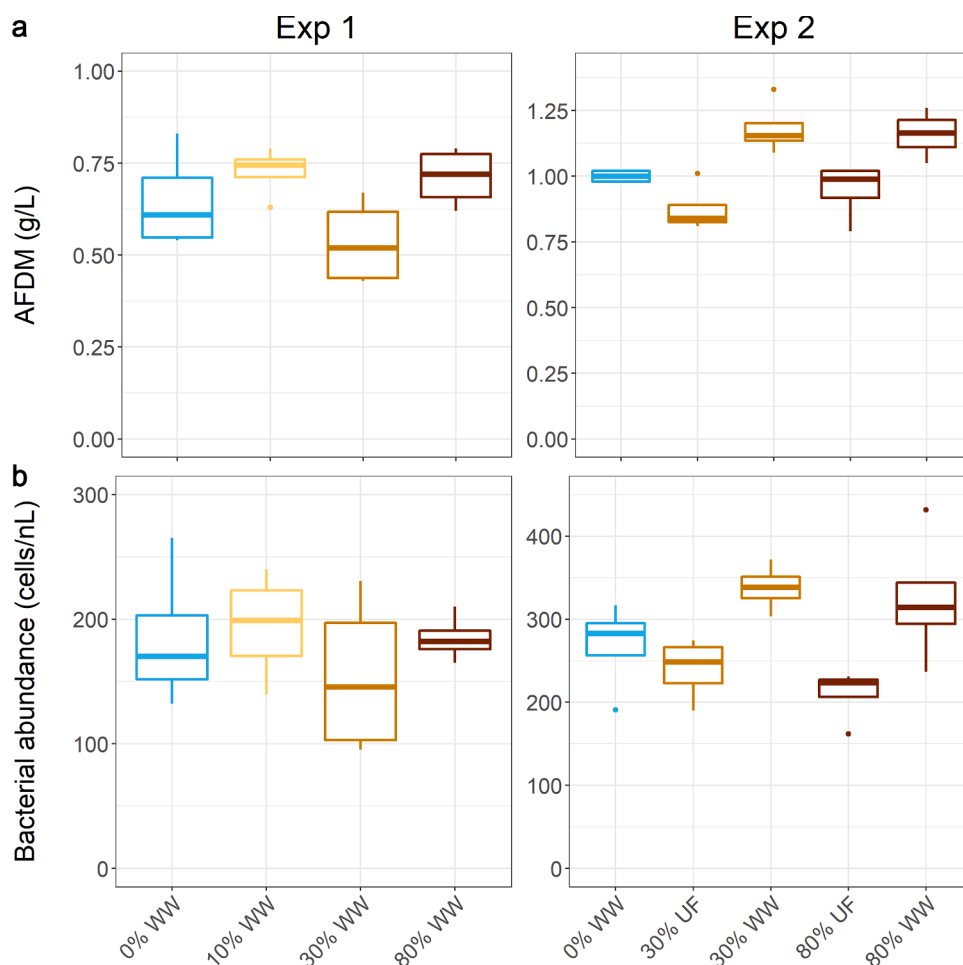


Fig. 2. Total biomass and bacterial abundance. a) Total biomass (i.e., ash-free dry mass, AFDM) and b) bacterial abundance of the BT samples at the beginning of the biotransformation experiments (Exp 1 and Exp 2). Values were determined for all replicates of the respective treatments ($n = 4$). Total biomass expressed as AFDM (g/L). Bacterial abundance expressed as flow cytometric cell counts (cells/nL). Box sizes correspond to the first and third quartiles (25% and 75% quartiles); whiskers extend to ± 1.5 times the interquartile range. Outliers are represented as dots.

biofilms at the beginning of the experiment (Fig. 2a) and a mean bacterial biomass of 179 ± 47 cells/nL (Fig. 2b). In Exp 1, biomass was comparable between treatments and no dependence of biomass with increasing WW-percentage was observable. In Exp 2, the mean total biomass and bacterial abundance was 1.03 ± 0.15 g/L and 276 ± 67 cells/nL, respectively. Here, a trend towards higher biomass in non-filtered versus ultrafiltered treatments was discernible. However, statistical analysis comparing the relative importance of biomass and treatment on k_{bio} confirmed that treatment conditions explained most of the variability in the rate constants for the chemicals showing the *downstream effect*, while biomass differences played only a minor role (SI section S2.2). We also compared biomass dynamics over the course of the experiments between the different treatments and between biotransformation (BT) batches and unspiked biological controls (BC; see SI sections S2.3 and S2.4). We found that biomass was dynamic but that dynamics were comparable between the treatments within experiments and between spiked and unspiked batches in both experiments.

3.4. MPs with highest influent concentrations typically showed highest removal in WWTP

In order to compare the removal of MPs in the WWTP to the biotransformation potential in the biofilms, we monitored influent and effluent concentrations of the *study compounds* in the WWTP producing

the treated effluent for our experiments (Fig. 3, lower panel). Based on these data, we calculated the percentage removal of the compounds that were found in measurable concentrations in the influent (Fig. 3, upper panel and SI section S3). Interestingly, the compounds that were removed to the highest extent ($> 80\%$) during wastewater treatment also were amongst those exhibiting the highest influent concentrations (> 1000 ng/L). Indeed, only a few compounds with comparably high influent concentrations (i.e., 4-/5-methyl-benzotriazole, benzotriazole and diclofenac in both experiments, and acesulfame and DEET in Exp 2) did not show removals $> 80\%$. However, it is to note that acesulfame and DEET still were removed by 77% and 59% during wastewater treatment in Exp 2, respectively, while the first three MPs were fully persistent during wastewater treatment in Exp 1 and showed removal of only 39%, 57% and 29% in Exp 2, respectively. Within the *study compounds*, the majority of MPs with influent concentrations < 1000 ng/L were removed to a lesser extent (i.e., $< 80\%$) during wastewater treatment, with the exception of mefenamic acid (Exp 1), mianserin (Exp 1), trifloxystrobin (Exp 1), and ranitidine (Exp 2). However, the measured concentrations of the last three were close to their respective LOQ and their calculated removal thus highly uncertain, leaving mefenamic acid as the sole clear exception with removal $> 80\%$ despite an influent concentration < 1000 ng/L for our *study compounds*.

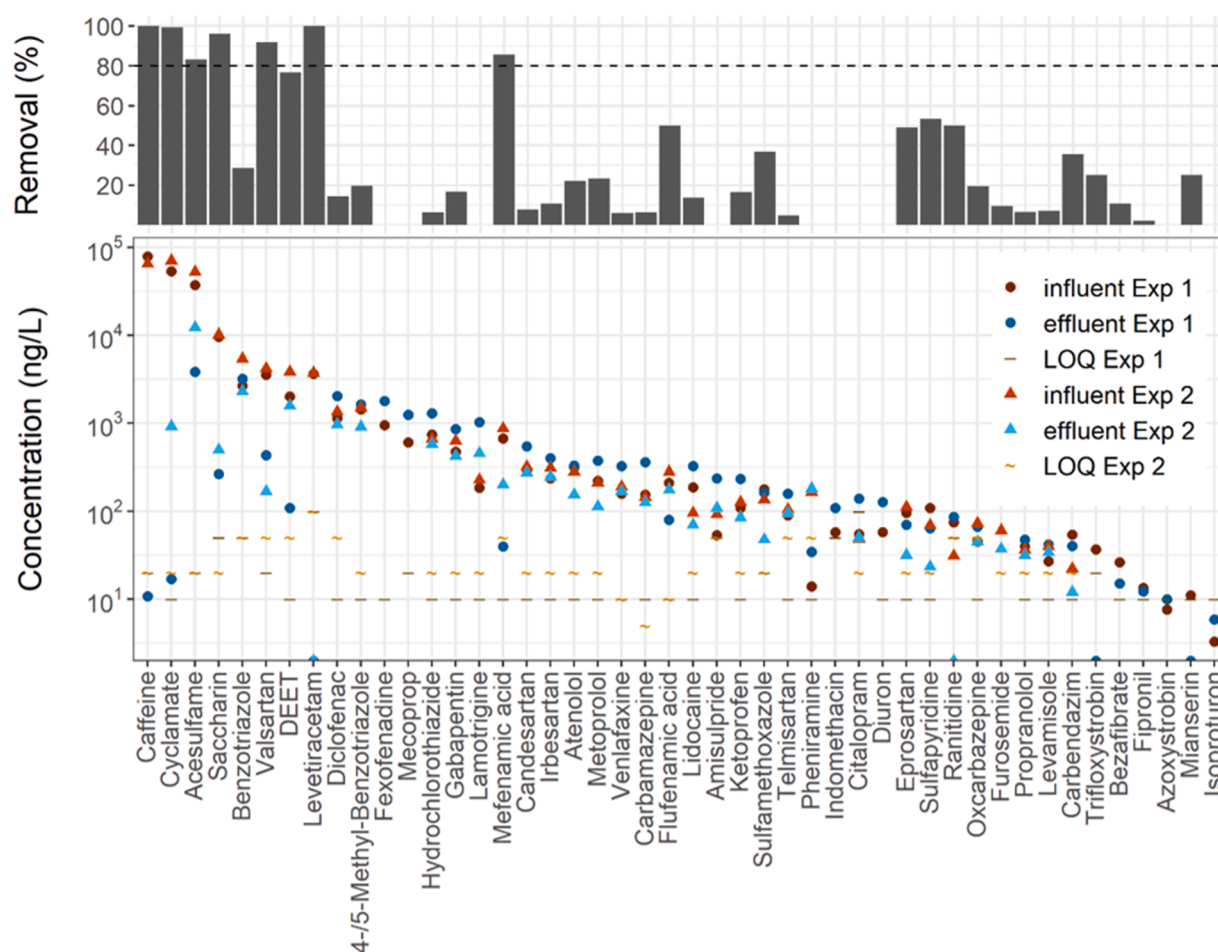


Fig. 3. Micropollutant concentrations and removal in the WWTP. All *study compounds* that were found in the WWTP influent ($n = 46$) during the biofilm cultivation phase of either Exp 1 and/or 2 are displayed. In the lower panel, the in- and effluent concentrations, as well as the analytical limits of quantification (LOQ) are given. Concentrations that were below the limit of detection are indicated as symbol lying on the x-axis. In the upper panel, the average percentage removal during wastewater treatment for the duration of the biofilm cultivation periods for Exp 1 and 2 is shown. For compounds showing an increasing concentration during wastewater treatment, no removal bar is depicted.

3.5. Identification of taxa aligning with downstream effect

Sequencing of the 16S rRNA gene was performed for biomass sampled from biofilms and WW from both experiments. Taxa present in WW and differently abundant in a given treatment compared to the control (0% WW) were selected from the 16S dataset of Exp 1 (Figure S31). We found 184 taxa originating from WW that followed a pattern of higher abundance with higher amounts of WW. In Exp 2, we found 202

taxa that also showed an increasing pattern with increasing WW, but which, relative to the 0% WW control, were not significantly more abundant in the UF treatments (Figure S31). Combining these two datasets lead to a final list of 146 taxa originating from wastewater whose abundance patterns followed the patterns in k_{bio} for the MPs showing the *downstream effect* (Fig. 4, for a complete list of these taxa see Table Appendix A8).

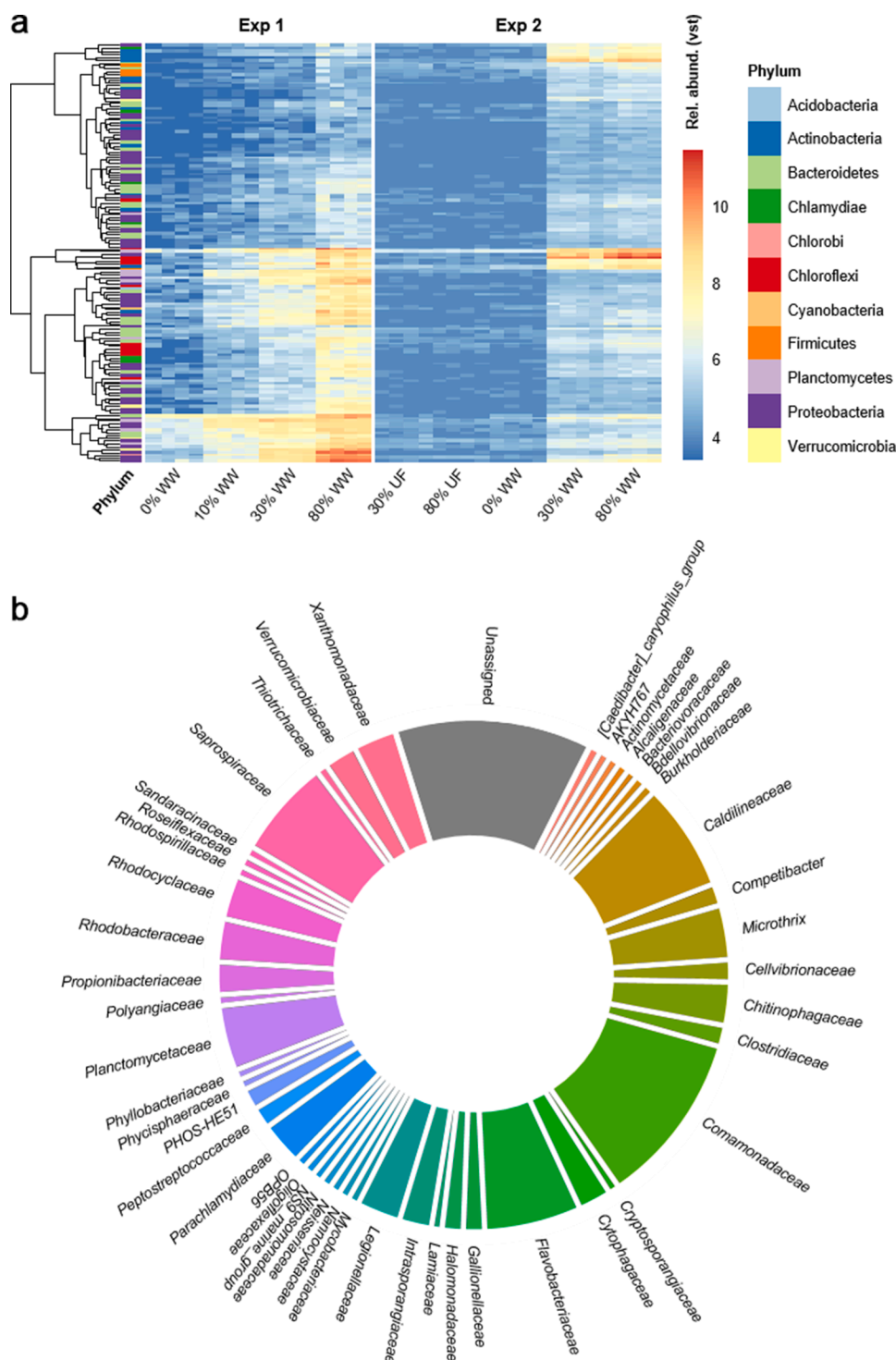


Fig. 4. Taxa following *downstream effect* as identified via 16S-pattern analysis. a) Heat map showing the relative abundance (with variance stabilizing transformation – vst) of the 146 taxa that followed the pattern in k_{bio} for the MPs showing the *downstream effect*. b) Repartition of the 146 taxa at the family level.

4. Discussion

With this study we aimed to elucidate the mechanisms underlying observations of increased MP biotransformation for a number of chemicals in biofilms grown downstream of WWTP outfalls relative to upstream biofilms ('downstream effect'). So far, our results clearly demonstrate that:

- 1) the *downstream effect* is reproducible under controlled conditions and scaled with the percentage of WW in Exp 1;
- 2) ultrafiltration (i.e., removal of particles and microorganisms deriving from the WWTP) prevented the *downstream effect* in Exp 2;

- 3) biotransformation was dictated by the microbial community composition (i.e., the treatment condition), rather than only by bacterial abundance in the batch experiments;
- 4) with very few exceptions, compounds that were removed to the highest extent (> 80%) in the WWTP also exhibited the highest influent concentrations (> 1000 ng/L);
- 5) 146 bacterial taxa showed abundance patterns that are consistent with the *downstream effect*.

By combining these key results, a nuanced picture emerges (Fig. 5). As can be seen in Fig. 5, we identified three major clusters (A, B and C) of

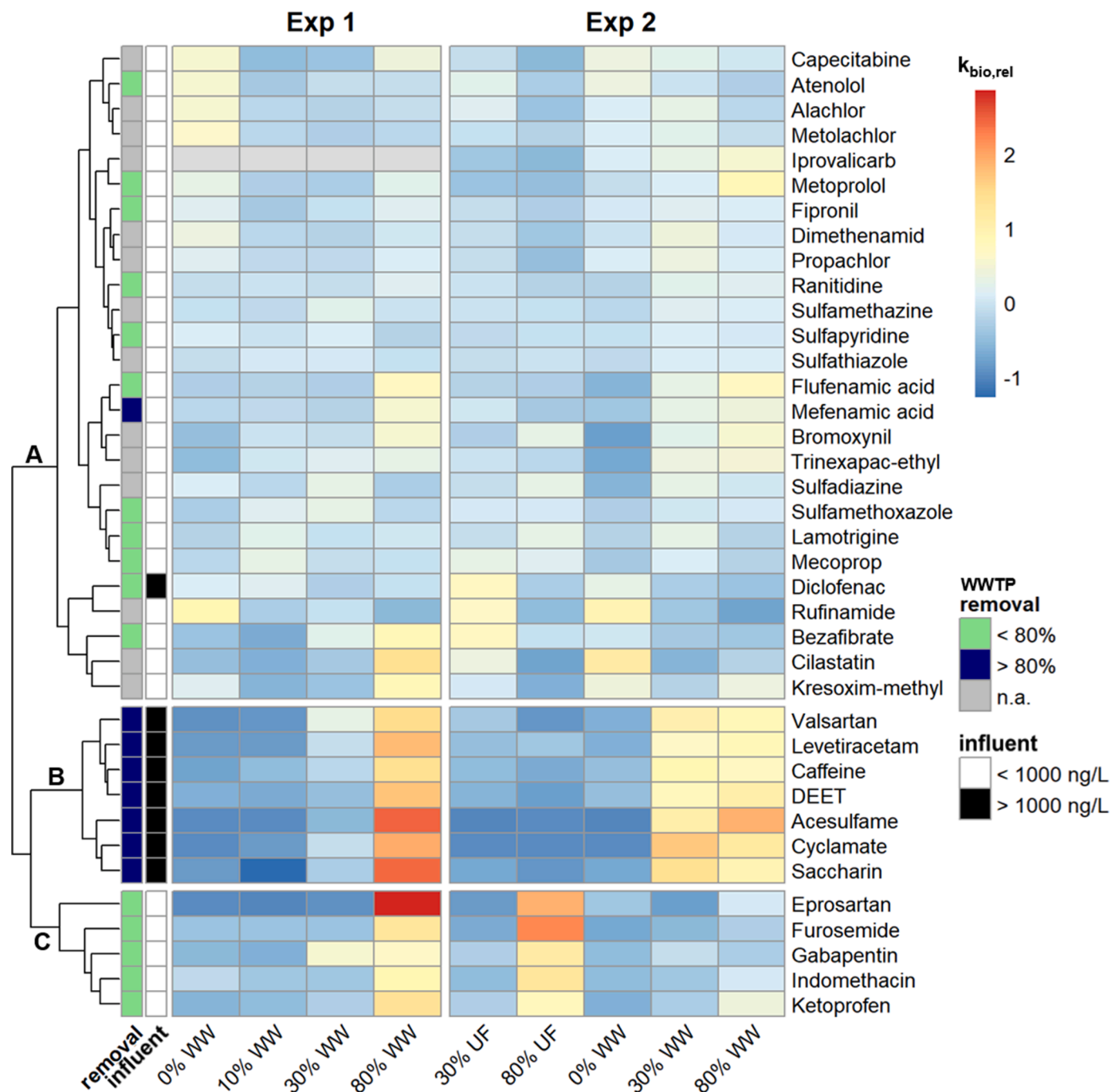


Fig. 5. Biotransformation trends. Heatmap displaying the fold-changes of the biotransformation rate constants determined in Exp 1 and Exp 2. The level-normalized biotransformation rate constants ($k_{bio,rel}$) are depicted for every substance that underwent biotransformation in at least one of the investigated treatment conditions. Hierarchical clustering was used to order the substances and split into three main clusters (A, B and C). Annotations on the left depict removal and influent concentrations of the respective substance measured during Exp 1 in the WWTP providing the effluent water for the experiments. The WWTP removal was denominated 'n.a.' for substances that were not detected in the influent.

MP biotransformation patterns based on the (level-normalized) k_{bio} values obtained for the different biofilm communities. Cluster A, which contained 26, and hence the majority of the 38 biotransformed compounds, was least influenced by the treatment conditions. It contained the majority of compounds that had not shown a *downstream effect* in our previous study and whose biotransformation seemed to largely align with bacterial abundance trends in our previous data (Desiante et al. 2021). This is in agreement with the fact that cluster A contains mostly compounds that are thought to be biotransformed by enzymes that are ubiquitous among living organisms or enzymes that are closely related to bacterial growth (Achermann et al. 2018a, Achermann et al. 2018b, Desiante et al. 2021, Johnson et al. 2015). All taken together, the findings from this and our previous study (Desiante et al. 2021) point toward co-metabolism – ‘the transformation of a non-growth substrate in the obligate presence of a growth substrate or another transformable compound’ – as the major biotransformation process for these compounds (Dalton and Stirling 1982).

Cluster A was separated from clusters B and C, which both contain compounds that showed a clear *downstream effect* in Exp 1 (Fig. 5). Of those, cluster B contains those seven compounds that show no *downstream effect* upon ultrafiltration in Exp 2, while cluster C contains five compounds that actually were removed, on average, to the highest extent in the 80% UF treatment in Exp 2. As can be seen from the information on influent concentrations and removal in the WWTP added as annotations in Fig. 5, all of the compounds in cluster B were present in high concentrations (> 1000 ng/L) in the influent to the WWTP and were removed to a large extent ($> 80\%$) during wastewater treatment. Interestingly, the five compounds previously shown to exhibit a *downstream effect* in natural streams (i.e., acesulfame, cyclamate, DEET, lev- etiracetam and saccharin) are all contained in cluster B (Desiante et al. 2021). We also note that diclofenac, the only compound with high influent concentrations but removal $< 80\%$ in both Exp 1 and Exp 2, does not fall into cluster B.

Combining all evidence from Exp 1 and Exp 2 suggests that the increased biotransformation capacity of the biofilms with increased percentage of wastewater (i.e., the *downstream effect*) observed for cluster B compounds is most likely caused directly by bacteria (or larger aggregates thereof) being released from the WWTP with the treated effluent. In principle, there are at least two mechanisms how this could influence the biotransformation capacity of the biofilms: i) The microorganisms being released with treated effluent capable of degrading the MPs in cluster B may either directly colonize the biofilms, or ii) their biotransformation traits may be transferred to other microorganisms growing in the biofilms, by, e.g., horizontal gene transfer. Based on the 16S data rRNA data, we identified 146 taxa that were present in WW, showed increasing abundances in biofilms with increasing WW proportion, and were filtered out by ultrafiltration. These findings confirmed that there are indeed bacterial taxa originating from the WWTP that can establish in biofilms growing downstream of WWTPs, as previously shown (Carles et al. 2021, Chonova et al. 2019, Mußmann et al. 2013). More importantly, these taxa exhibited relative abundance patterns across Exp 1 and Exp 2 that follow patterns of relative biotransformation rate constants for compounds showing the *downstream effect*, i.e., cluster B compounds. Consequently, it may be speculated that some of these taxa were involved in the degradation of cluster B compounds.

It is now interesting to further note that the compounds in cluster B exclusively exhibit both high influent concentrations to and high removal in the WWTP. In combination with the fact that the capacity to degrade these compounds in biofilms is dependent on WW-borne particles filtered out by ultrafiltration, our results therefore suggest that the *downstream effect* is not only caused by microorganisms originating from the WWTP, but that these microorganisms have adapted to biotransform the specific compounds in cluster B, which reach the WWTP in comparably high concentrations of > 1000 ng/L. With respect to the main aim of this study, i.e., to elucidate the mechanisms underlying the increased

MP biotransformation potential of biofilms grown downstream of WWTPs, we can therefore further conclude that the *downstream effect* is mostly due to those adapted microorganisms integrating into downstream biofilms and/or transferring their increased biotransformation capacity to the biofilms. In turn, at least for compounds in cluster B, this falsifies the hypothesis that elevated MP concentrations from WWTP effluents and in-situ adaptation in the river itself explain the increased biotransformation in downstream biofilms. It needs to be noted though that the biofilm colonization period in our experiments was only four weeks. While the biofilms did reach a mature stage during that time, time series experiments would be required to definitely exclude any long-term effects of in-stream exposure to MPs on the downstream biofilms' biodegradation capacity.

In support of our interpretation, evolutionary adaptation of bacteria in WWTPs has been previously shown for the compound acesulfame, whose biotransformation during activated sludge treatment suddenly emerged around the year 2010, while it has previously been considered a conservative tracer compound (Castronovo et al. 2017, Kahl et al. 2018, Kleinstaub et al. 2019). Also, evidence from previous field studies in combination with the fact that the compounds in cluster B are commonly amongst the best removed compounds in different WWTPs confirms that the phenomenon, at least for some of the compounds, is observable across different WWTPs and downstream river environments (Buerge et al. 2009, Castronovo et al. 2017, Coll et al. 2020, Desiante et al. 2021, Gurke et al. 2015, Margot et al. 2015, Seller et al. 2020). Moreover, having performed the two experiments in different seasons (i. e., summer 2019 and late winter 2020) confirms that our findings are also robust on a temporal scale.

An interesting follow-up question that arises from our observations is how this adaptation occurred in the WWTP in the first place and why exactly for the seven compounds in cluster B. Is it mostly due to the high influent concentrations that part of the activated sludge microbial consortium have adapted to and use as steady sources of carbon or other nutrients? Or to what extent is it related to the chemical structures of the compounds, e.g., by all of those compounds sharing certain metabolic pathways? As can be seen from Fig. 6, there is no single functional group that unites all of these compounds, yet, they all contain either an amide or sulfonamide substructure that could potentially be hydrolyzed by enzymes belonging to the amidohydrolase family. While, to the best of our knowledge, enzymatic reaction mechanisms that are involved in the biotransformation of these compounds in stream biofilms have not yet been investigated, there are several studies investigating reaction pathways and enzymes involved in the biotransformation of these compounds in pure or enrichment cultures (Fig. 6). For acesulfame, for instance, there is evidence for full catabolic biodegradation in activated sludge (Castronovo et al. 2017), enriched microbial consortia, as well as isolated bacterial species of the genera *Bosea* and *Chelatococcus* (Huang et al. 2021, Kleinstaub et al. 2019), and it has been suggested that the pathway involves formation of sulfamic acid and acetoacetate through sequential action of a sulfohydrolase and an amidohydrolase enzyme (Kleinstaub et al. 2019). Cyclamate has been shown to be transformed by the enzyme cyclamate sulfamatase, extracted from *Pseudomonas* sp., to form cyclohexylamine and sulfate (Nimura et al. 1974). In contrast to these initial hydrolytic transformations, for the other compounds mostly initial oxidative transformations have been reported. Saccharin has been proposed to be biotransformed to the compound catechol in a two-step process involving the enzyme saccharin dioxygenase, in *Sphingomonas xenophaga* SKN (Schleheck and Cook 2003). For the biotransformation of DEET, three enzymatic pathways were suggested, involving a hydrolase encoded on a gene found in *Pseudomonas putida* DTB, and a monooxygenase- and a dehydrogenase-pathway (Helbling et al. 2010b, Rivera-Cancel et al. 2007). For caffeine, two pathways have been proposed, the first involving demethylases found in plants, bacteria and fungi, and the second involving a caffeine (1,3,7-trimethylxanthine) oxidase from *Klebsiella* and *Rhodococcus* (Hakil et al. 1998, Madyastha et al. 1999, Mazzafera 2004). While for valsartan and levetiracetam no

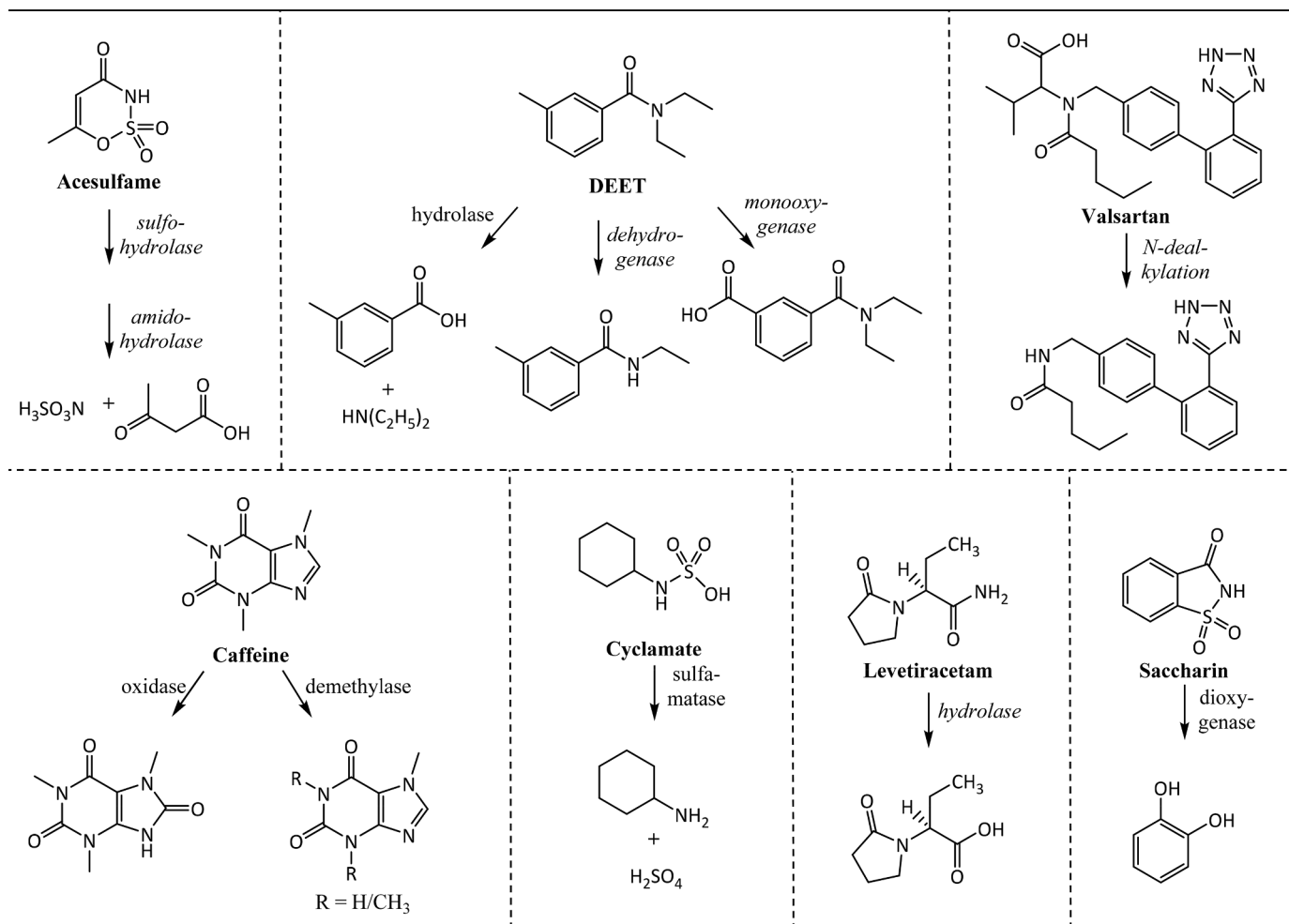


Fig. 6. Suggested transformation pathways of the seven compounds showing the *downstream effect*. Proposed enzymatic pathways from literature are displayed for the compounds acesulfame, caffeine, DEET, cyclamate, levetiracetam, saccharin and valsartan. Enzymatic pathways given in italics were only confirmed by transformation product analysis. Literature references to the respective pathways are given in the text.

pure or enrichment culture data detailing involved enzymes or taxa are available, transformation product analysis from activated sludge studies suggests that valsartan transformation is primarily initiated through oxidative N-dealkylation whereas the primary amide levetiracetam is primarily enzymatically hydrolyzed (Helbling et al. 2010a).

Overall, the pathway information gathered so far does not support the notion of a shared initial biotransformation reaction for the seven compounds in cluster B, which is further supported by the fact that the onset of biotransformation is observed at different percentages of WW in Exp 1 for the different compounds. In turn, this suggests the elevated WWTP influent concentrations as possible alternative explanation for the adaptation to degrade cluster B compounds. Indeed, concepts of WWTP biotechnology stipulate that the growth rate needs to exceed the loss rate (i.e., from withdrawal of excess sludge and with the effluent) for bacteria with a specific metabolic capacity to establish in an activated sludge process. Since growth rates of specific degraders depend on substrate concentration, it has been proposed, as early as in 1994, that percentage removal in WWTPs and half-lives in downstream aquatic environments can be predicted based on influent concentrations (Blok 1994). However, only very recently a correlation between biotransformation rate constants in WWTPs and WWTP influent concentrations has actually been demonstrated based on monitoring data for a large and diverse set of MPs (Nolte et al. 2020). Also, more recent data from studies using compound-specific isotope analysis experimentally demonstrated that mass transfer limitations may prevent catabolic

degradation of MPs below a certain concentration limit in the low $\mu\text{g/L}$ range (Kundu et al. 2019, Sun et al. 2021). This is consistent with earlier studies on the concentration-dependence of biodegradation kinetics of two herbicides that revealed a threshold of approximately 1 – 10 $\mu\text{g/L}$ above which growth of specific degrader biomass was observed (Toräng et al. 2003). In our study, the data suggests that the concentration limit for compounds showing the *downstream effect* lies in the range of 1 $\mu\text{g/L}$. Yet, at the same time, there was also one compound reaching the WWTP in concentrations above 1 $\mu\text{g/L}$ that did not show high removal in the WWTP (i.e., diclofenac), and, consistently, also did not show a *downstream effect*, confirming that concentration limits for metabolic degradation are substrate-specific and/or that certain compounds may be fully recalcitrant to biodegradation even at high concentrations (Schwarzenbach et al. 2005).

The lack of high WWTP influent concentrations and their lower removal in the WWTP might also offer a key to understanding the deviating behavior of compounds in cluster C. While they show a *downstream effect*, this effect is not removed through ultrafiltration, at least not at 80% WW. Contrasting this with cluster B behavior, these findings suggest that mechanisms other than the release of adapted degrader bacteria must underlie the *downstream effect* for cluster C compounds. Indeed, for these compounds, observations are more consistent with a direct effect of in-stream exposure to MPs on the periphyton.

Overall, our results suggest that community composition drives the

biotransformation patterns we observed for cluster B compounds. To shed some more light on what specific taxa might potentially be involved in biodegrading individual cluster B compounds, we searched the 146 taxa whose abundance patterns align with the downstream effect for high sequence similarity with species previously reported to degrade compounds showing the *downstream effect* (see Table S6 and SI Section S4). One notable finding from this analysis was a taxon annotated as *SM1A02* from the family *Phycisphaeraceae*, whose abundance pattern was fully consistent with the rate constant pattern of cluster B compounds and which showed strong and significant fold-changes between 0 and 80% WW in Exp 1 and 2 (\log_2 fold-change > 4; Table Appendix A8). These taxa have been shown to dominate acesulfame-degrading communities enriched from the activated sludge of six municipal wastewater treatment plants (Huang et al. 2021) and bioreactors with emerging acesulfame degradation capacity (unpublished data). Recent sequencing data also reported on the presence of putative sulfohydrolase genes in microalgae-associated *Phycisphaeraceae* sp., thus confirming the potential role of *SM1A02* in acesulfame degradation in biofilm communities (Rambo et al. 2020). These results support the notion that some of the 146 taxa revealed through pattern analysis indeed may be involved in degradation of compounds from cluster B. Yet, such hypotheses emerging from the data still need to be confirmed by complementary approaches such as culture/isolation methods and identification/quantification of functional genes related to biodegradation processes.

5. Conclusions

Two major implications arise from the results of our study:

- First, we provide clear experimental evidence that non-disinfected WWTP effluents change an ecological function of downstream biofilms, in this case their biotransformation potential. While this seems overall beneficial in the case of biotransformation since it contributes to lowering exposure to MPs in biofilms and, hence, in the overall stream environment, it raises the question what other functional changes might occur in biofilms exposed to treated WW. For instance, our results, which demonstrate the transfer of bacteria adapted to degrade MPs from the WWTP into stream biofilms and the establishment of that degradation capacity in those biofilms, suggest that it is likely that transfer of resistant bacteria and/or resistance genes also support the transfer of AR factors from WWTPs into biofilms (Abe et al. 2020, Balcázar 2018, Marti et al. 2013, Woegebauer et al. 2020). Similarly, another resistance mechanism, i.e., pollution-induced community tolerance of biofilms against MPs, has previously been shown to be elevated downstream of WWTPs (Corcoll et al. 2014, Tili et al. 2016, Tili et al. 2017) and to increase with increasing proportions of WW, especially for the phototrophic compartment of biofilm communities (Carles et al. 2021). It has been hypothesized that the increased tolerance is caused by the MPs released with the WWTP effluents, exerting a selective pressure on downstream communities, resulting in the extinction of sensitive and establishment of tolerant species. However, our results support a second plausible hypothesis, i.e., that the increase in tolerance in downstream biofilms might be due to integration of already tolerant species released with the WW or, more indirectly, due to changes in the biofilm communities that endow increased tolerance to the phototrophic community members through yet unknown mechanisms.
- Second, our study revealed distinct differences in MP degradation patterns amongst biofilms grown with different proportions of non-disinfected WW for compounds potentially undergoing metabolic degradation versus those more likely undergoing co-metabolic biotransformation. The type of mesocosm experiments introduced here could therefore become a useful tool to distinguish co-metabolically from metabolically degraded compounds in a highly

environmentally relevant setting. This will allow studying questions of fundamental interest in environmental chemistry such as how molecular structure influences which compounds can be metabolically degraded in the environment and at what concentrations, or which families of microbes are most likely to be involved in such metabolic degradation. Such information is essential in order to design compounds that are readily biodegradable in a river environment or to promote growth of specific degrading strains in bioremediation efforts, to finally reduce anthropogenic pollution in our environment.

Declaration of Competing Interest

The authors declare that they have no known competing financial interests or personal relationships that could have appeared to influence the work reported in this paper.

Acknowledgments

The authors thank Richard Fankhauser (Eawag) for helping to build and maintain the Maiandros system, Denise Freudemann and the AuA lab (Eawag) for their support in analysis of the water physicochemical parameters and the EcoImpact team (Eawag) for fruitful discussions. Andreas Scheidegger (Eawag) is acknowledged for discussion on statistical models. Reto Britt (Eawag), Franziska Jud (Eawag), Christelle Oltramare (Eawag) and Silvano Murk (Eawag) are acknowledged for their support in performing the biotransformation experiments. This work was financially supported by the European Research Council under the European Union's Seventh Framework Programme (ERC grant agreement no. 614768, PROduCTS) and by the project EcoImpact 2.0 funded through Eawag Discretionary Funds.

Correspondence and material requests should be addressed to K. F.

Supplementary materials

Supplementary material associated with this article can be found, in the online version, at doi:[10.1016/j.watres.2022.118413](https://doi.org/10.1016/j.watres.2022.118413).

References

- Abe, K., Nomura, N., Suzuki, S., 2020. fiao031. Biofilms: hot spots of horizontal gene transfer (HGT) in aquatic environments, with a focus on a new HGT mechanism. *FEMS Microbiol. Ecol.* 96 (5).
- Achermann, S., Bianco, V., Mansfeldt, C.B., Vogler, B., Kolvenbach, B.A., Corvini, P.F.X., Fenner, K., 2018a. Biotransformation of Sulfonamide Antibiotics in Activated Sludge: The Formation of Pterin-Conjugates Leads to Sustained Risk. *Environ. Sci. Technol.* 52 (11), 6265–6274.
- Achermann, S., Falas, P., Joss, A., Mansfeldt, C.B., Men, Y., Vogler, B., Fenner, K., 2018b. Trends in Micropollutant Biotransformation along a Solids Retention Time Gradient. *Environ. Sci. Technol.* 52 (20), 11601–11611.
- Andrews, S. (2010) FastQC: a quality control tool for high throughput sequence data.
- Balcázar, J.L., 2018. How do bacteriophages promote antibiotic resistance in the environment? *Clin. Microbiol. Infect.* 24 (5), 447–449.
- Blok, J., 1994. Extrapolation of Biodegradability Test Data by Use of Growth Kinetic-Parameters. *Ecotoxicol. Environ. Saf.* 27 (3), 306–315.
- Buerge, I.J., Buser, H.R., Kahle, M., Muller, M.D., Poiger, T., 2009. Ubiquitous Occurrence of the Artificial Sweetener Acesulfame in the Aquatic Environment: An Ideal Chemical Marker of Domestic Wastewater in Groundwater. *Environ. Sci. Technol.* 43 (12), 4381–4385.
- Burdon, F.J., Bai, Y.H., Reyes, M., Tamminen, M., Staudacher, P., Mangold, S., Singer, H., Rasanen, K., Joss, A., Tiegs, S.D., Jokela, J., Eggen, R.I.L., Stamm, C., 2020. Stream microbial communities and ecosystem functioning show complex responses to multiple stressors in wastewater. *Global Change Biol.* 26 (11), 6363–6382.
- Caliman, F.A., Gavrilescu, M., 2009. Pharmaceuticals, Personal Care Products and Endocrine Disrupting Agents in the Environment - a Review. *Clean-Soil Air Water* 37 (4-5), 277–303.
- Callahan, B.J., McMurdie, P.J., Holmes, S.P., 2017. Exact sequence variants should replace operational taxonomic units in marker-gene data analysis. *ISME J.* 11 (12), 2639–2643.
- Carles, L., Wulschleger, S., Joss, A., Eggen, R.I.L., Schirmer, K., Schuwirth, N., Stamm, C., Tili, A., 2021. Impact of wastewater on the microbial diversity of periphyton and its tolerance to micropollutants in an engineered flow-through channel system. *Water Res.* 203, 117486.

- Castronovo, S., Wick, A., Scheurer, M., Nodler, K., Schulz, M., Ternes, T.A., 2017. Biodegradation of the artificial sweetener acesulfame in biological wastewater treatment and sandfilters. *Water Res.* 110, 342–353.
- Chonova, T., Kurmayer, R., Rimet, F., Labanowski, J., Vasselon, V., Keck, F., Illmer, P., Bouchez, A., 2019. Benthic Diatom Communities in an Alpine River Impacted by Waste Water Treatment Effluents as Revealed Using DNA Metabarcoding. *Front. Microbiol.* 10.
- Coll, C., Bier, R., Li, Z., Langenheder, S., Gorokhova, E., Sobek, A., 2020. Association between Aquatic Micropollutant Dissipation and River Sediment Bacterial Communities. *Environ. Sci. Technol.* 54 (22), 14380–14392.
- Collignon, P., Beggs, J.J., Walsh, T.R., Gandra, S., Laxminarayan, R., 2018. Anthropological and socioeconomic factors contributing to global antimicrobial resistance: a univariate and multivariable analysis. *Lancet Planet Health* 2 (9), e398–e405.
- Corcoll, N., Acuna, V., Barcelo, D., Casellas, M., Guasch, H., Huerta, B., Petrovic, M., Ponsati, L., Rodriguez-Mozaz, S., Sabater, S., 2014. Pollution-induced community tolerance to non-steroidal anti-inflammatory drugs (NSAIDs) in fluvial biofilm communities affected by WWTP effluents. *Chemosphere* 112, 185–193.
- Dalton, H., Stirling, D.I., 1982. Co-metabolism. *Philos. Trans. R Soc. Lond. B Biol. Sci.* 297, 481–496, 1088.
- Desiante, W.L., Minas, N.S., Fenner, K., 2021. Micropollutant biotransformation and bioaccumulation in natural stream biofilms. *Water Res.* 193, 116846.
- Fenner, K., Canonica, S., Wackett, L.P., Elsner, M., 2013. Evaluating pesticide degradation in the environment: blind spots and emerging opportunities. *Science* 341 (6147), 752–758.
- FOEN, F.O.f.t.E. (2020) National River Monitoring and Survey Programme (NADUF) [WWW Document].
- Gavrilescu, M., Demnerova, K., Aamand, J., Agathos, S., Fava, F., 2015. Emerging pollutants in the environment: present and future challenges in biomonitoring, ecological risks and bioremediation. *N Biotechnol.* 32 (1), 147–156.
- Gurke, R., Rossmann, J., Schubert, S., Sandmann, T., Röbler, M., Oertel, R., Fauler, J., 2015. Development of a SPE-HPLC-MS/MS method for the determination of most prescribed pharmaceuticals and related metabolites in urban sewage samples. *J. Chromatogr. B* 990, 23–30.
- Hakil, M., Denis, S., Viniegra-Gonzalez, G., Augur, C., 1998. Degradation and product analysis of caffeine and related dimethylxanthines by filamentous fungi. *Enzyme Microb. Technol.* 22 (5), 355–359.
- Helbling, D.E., Hollender, J., Kohler, H.P.E., Fenner, K., 2010a. Structure-Based Interpretation of Biotransformation Pathways of Amide-Containing Compounds in Sludge-Seeded Bioreactors. *Environ. Sci. Technol.* 44 (17), 6628–6635.
- Helbling, D.E., Hollender, J., Kohler, H.P.E., Singer, H., Fenner, K., 2010b. High-Throughput Identification of Microbial Transformation Products of Organic Micropollutants. *Environ. Sci. Technol.* 44 (17), 6621–6627.
- Herlemann, D.P.R., Labrenz, M., Jürgens, K., Bertilsson, S., Waniek, J.J., Andersson, A.F., 2011. Transitions in bacterial communities along the 2000 km salinity gradient of the Baltic Sea. *ISME J.* 5 (10), 1571–1579.
- Huang, Y., Deng, Y., Law, J.C.-F., Yang, Y., Ding, J., Leung, K.S.-Y., Zhang, T., 2021. Acesulfame aerobic biodegradation by enriched consortia and *Chelatococcus* spp.: Kinetics, transformation products, and genomic characterization. *Water Res.* 202, 117454.
- Johnson, D.R., Helbling, D.E., Lee, T.K., Park, J., Fenner, K., Kohler, H.P., Ackermann, M., 2015. Association of biodiversity with the rates of micropollutant biotransformations among full-scale wastewater treatment plant communities. *Appl. Environ. Microbiol.* 81 (2), 666–675.
- Ju, F., Beck, K., Yin, X., Maccagnan, A., McDardell, C.S., Singer, H.P., Johnson, D.R., Zhang, T., Bürgmann, H., 2019. Wastewater treatment plant resistomes are shaped by bacterial composition, genetic exchange, and upregulated expression in the effluent microbiomes. *ISME J.* 13 (2), 346–360.
- Kahl, S., Kleinstaub, S., Nivala, J., van Afferden, M., Reemtsma, T., 2018. Emerging Biodegradation of the Previously Persistent Artificial Sweetener Acesulfame in Biological Wastewater Treatment. *Environ. Sci. Technol.* 52 (5), 2717–2725.
- Kleinstaub, S., Rohwerder, T., Lohse, U., Seiwert, B., Reemtsma, T., 2019. Sated by a Zero-Calorie Sweetener: Wastewater Bacteria Can Feed on Acesulfame. *Front. Microbiol.* 10, 2606.
- Kolde, R. (2015) Pheatmap: pretty heatmaps. R package version 1.0.12 <https://CRAN.R-project.org/package=pheatmap>.
- Kundu, K., Marozava, S., Ehrl, B., Merl-Pham, J., Griebler, C., Elsner, M., 2019. Defining lower limits of biodegradation: atrazine degradation regulated by mass transfer and maintenance demand in *Arthrobacter aurescens* TC1. *ISME J.* 13 (9), 2236–2251.
- Latino, D.A.R.S., Wicker, J., Gütlein, M., Schmid, E., Kramer, S., Fenner, K., 2017. Eawag-Soil in envPath: a new resource for exploring regulatory pesticide soil biodegradation pathways and half-life data. *Environ. Sci.* 19 (3), 449–464.
- Lee, J., Ju, F., Maile-Moskowitz, A., Beck, K., Maccagnan, A., McDardell, C.S., Molin, M. D., Fenicia, F., Vikesland, P., Pruden, A., Stamm, C., Bürgmann, H., 2021. Unraveling the riverine antibiotic resistome: the downstream fate of anthropogenic inputs. *Water Research*, 117050.
- Madyastha, K.M., Sridhar, G.R., Vadiraja, B.B., Madhavi, Y.S., 1999. Purification and partial characterization of caffeine oxidase—a novel enzyme from a mixed culture consortium. *Biochem. Biophys. Res. Commun.* 263 (2), 460–464.
- Magoč, T., Salzberg, S.L., 2011. FLASH: fast length adjustment of short reads to improve genome assemblies. *Bioinformatics* 27 (21), 2957–2963.
- Margot, J., Rossi, L., Barry, D.A., Holliger, C., 2015. A review of the fate of micropollutants in wastewater treatment plants. *Wiley Interdiscip. Rev.* 2 (5), 457–487.
- Marti, E., Jofre, J., Balcasar, J.L., 2013. Prevalence of antibiotic resistance genes and bacterial community composition in a river influenced by a wastewater treatment plant. *PLoS One* 8 (10), e78906.
- Martin, M. (2011) Cutadapt removes adapter sequences from high-throughput sequencing reads. 2011 17(1), 3.
- Mazzafera, P., 2004. Catabolism of caffeine in plants and microorganisms. *Front. Biosci.* 9, 1348–1359.
- Munz, N.A., Burdon, F.J., de Zwart, D., Junghans, M., Melo, L., Reyes, M., Schonenberger, U., Singer, H.P., Spycher, B., Hollender, J., Stamm, C., 2017. Pesticides drive risk of micropollutants in wastewater-impacted streams during low flow conditions. *Water Res.* 110, 366–377.
- Mußmann, M., Ribot, M., von Schiller, D., Merbt, S.N., Augspurger, C., Karwautz, C., Winkel, M., Battin, T.J., Marti, E., Daims, H., 2013. Colonization of freshwater biofilms by nitrifying bacteria from activated sludge. *FEMS Microbiol. Ecol.* 85 (1), 104–115.
- Nimura, T., Tokieda, T., Yamaha, T., 1974. Partial purification and some properties of cyclamate sulfamylase. *J. Biochem.* 75 (2), 407–417.
- Nolte, T.M., Chen, G., van Schayk, C.S., Pinto-Gil, K., Hendriks, A.J., Peijnenburg, W., Ragas, A.M.J., 2020. Disentanglement of the chemical, physical, and biological processes aids the development of quantitative structure-biodegradation relationships for aerobic wastewater treatment. *Sci. Total Environ.* 708, 133863.
- Posthuma, L., Zijp, M.C., De Zwart, D., Van de Meent, D., Globevnik, L., Koprivsek, M., Focks, A., Van Gils, J., Birk, S., 2020. Chemical pollution imposes limitations to the ecological status of European surface waters. *Sci. Rep.* 10 (1), 14825.
- Core Team, R., 2017. A language and environment for statistical computing. R. Foundation for Statistical Computing, Vienna, Austria. URL <https://www.R-project.org/>.
- Rambo, I.M., Dombrowski, N., Constant, L., Erdner, D., Baker, B.J., 2020. Metabolic relationships of uncultured bacteria associated with the microalgae *Gambierdiscus*. *Environ. Microbiol.* 22 (5), 1764–1783.
- Rivera-Cancel, G., Bocioaga, D., Hay, A.G., 2007. Bacterial degradation of N,N-diethyl-m-toluamide (DEET): cloning and heterologous expression of DEET hydrolase. *Appl. Environ. Microbiol.* 73 (9), 3105–3108.
- Schleheck, D., Cook, A.M., 2003. Saccharin as a sole source of carbon and energy for *Sphingomonas xenophaga* SKN. *Arch. Microbiol.* 179 (3), 191–196.
- Schmieder, R., Edwards, R., 2011. Quality control and preprocessing of metagenomic datasets. *Bioinformatics* 27 (6), 863–864.
- Schwarzenbach, R.P., Gschwend, P.M., Imboden, D.M., 2005. Environmental organic chemistry. John Wiley & Sons.
- Seller, C., Honti, M., Singer, H., Fenner, K., 2020. Biotransformation of Chemicals in Water–Sediment Suspensions: Influencing Factors and Implications for Persistence Assessment. *Environ. Sci. Technol. Lett.* 7 (11), 854–860.
- Stamm, C., Räsänen, K., Burdon, F.J., Altermatt, F., Jokela, J., Joss, A., Ackermann, M., Eggen, R.L.L., 2016. In: Dumbrell, A.J., Kordas, R.L., Woodward, G. (Eds.), *Adv. Ecol. Res.* 183–223 (eds), pp.
- Stewart, T.J., Behra, R., Sigg, L., 2015. Impact of chronic lead exposure on metal distribution and biological effects to periphyton. *Environ. Sci. Technol.* 49 (8), 5044–5051.
- Sun, F., Mellage, A., Gharasoo, M., Melsbach, A., Cao, X., Zimmermann, R., Griebler, C., Thullner, M., Cirpka, O.A., Elsner, M., 2021. Mass-Transfer-Limited Biodegradation at Low Concentrations—Evidence from Reactive Transport Modeling of Isotope Profiles in a Bench-Scale Aquifer. *Environ. Sci. Technol.* 55 (11), 7386–7397.
- Tlili, A., Berard, A., Blanck, H., Bouchez, A., Cássio, F., Eriksson, K.M., Morin, S., Montuelle, B., Navarro, E., Pascoal, C., Pesce, S., Schmitt-Jansen, M., Behra, R., 2016. Pollution-induced community tolerance (PACT): towards an ecologically relevant risk assessment of chemicals in aquatic systems. *Freshwater Biol.* 61 (12), 2141–2151.
- Tlili, A., Hollender, J., Kienle, C., Behra, R., 2017. Micropollutant-induced tolerance of in situ periphyton: Establishing causality in wastewater-impacted streams. *Water Res.* 111, 185–194.
- Toräng, L., Nyholm, N., Albrechtsen, H.J., 2003. Shifts in biodegradation kinetics of the herbicides MCPP and 2,4-D at low concentrations in aerobic aquifer materials. *Environ. Sci. Technol.* 37 (14), 3095–3103.
- van den Berg, R.A., Hoefsloot, H.C., Westerhuis, J.A., Smilde, A.K., van der Werf, M.J., 2006. Centering, scaling, and transformations: improving the biological information content of metabolomics data. *BMC Genomics* 7, 142.
- Wang, Y., Lai, A., Latino, D., Fenner, K., Helbling, D.E., 2018. Evaluating the environmental parameters that determine aerobic biodegradation half-lives of pesticides in soil with a multivariable approach. *Chemosphere* 209, 430–438.
- Wen, Y.R., Schoups, G., van de Giesen, N., 2017. Organic pollution of rivers: Combined threats of urbanization, livestock farming and global climate change. *Sci. Rep.* 7.
- Wickham, H., 2016. ggplot2: Elegant Graphics for Data Analysis. Springer-Verlag New York. Available from: <https://ggplot2.tidyverse.org>.
- Woegerbauer, M., Bellanger, X., Merlin, C., 2020. Cell-Free DNA: An Underestimated Source of Antibiotic Resistance Gene Dissemination at the Interface Between Human Activities and Downstream Environments in the Context of Wastewater Reuse. *Front. Microbiol.* 11 (671).